Non-linear Dead-time Error Compensation Method of Dual Active Bridge DC-DC Converter for Variable DC-bus Voltage

Jun-ichi Itoh, Kengo Kawauchi, Hiroki Watanabe
Dept. of Electrical, Electronics and Information Engineering
Nagaoka University of Technology
Niigata, Japan
itoh@vos.nagaokaut.ac.jp, k_kawauchi@stn.nagaokaut.ac.jp, hwatanabe@vos.nagaokaut.ac.jp

Abstract— **This paper proposes a transmission power error compensation method for a Dual Active Bridge (DAB) converter with a three-level operation when a DC-bus is varied. The non-linear transmission power error due to a dead-time is compensated by designing a zero current period to be longer than the dead-time using the three-level operation because the non-linear transmission power error occurs when an inductor current reaches zero during the dead-time. The proposed method adjusts a zero-voltage period according to the variable DC-bus voltage in order to design the zero current period for compensating the non-linear transmission power error. In addition, the three-level operation is controlled to reduce a circulating current in order to reduce RMS value of the inductor current. The validity of the proposed method is confirmed by a 1.9-kW prototype. As the experimental results, the transmission power error is reduced from 49% to 3.5%.**

Keywords— Dual Active Bridge converter; Dead-time error; Three-level operation;

I. INTRODUCTION

In recent years, DC micro-grid systems have been actively researched in order to solve environmental problem [1-3]. In the DC micro-grid systems, energy storage systems is necessary in order to compensate the power fluctuation of the high voltage DC-bus because the generated power depends on the meteorological condition. In order to control power and isolate between the high voltage DC-bus and a buttery for safety, a bi-directional isolated DC-DC converter is applied. A dual active bridge (DAB) converter is generally employed because the DAB converter has a good feature in efficiency [4-7]. In particular, the DAB converter achieves a zero voltage switching (ZVS) without any additional components. However, a transmission power error occurs due to a non-linear dead-time at light load to medium load although the DAB converter has to operate at wide load range [8]. The non-linear transmission power error occurs due to a voltage polarity reversal phenomenon. This phenomenon is caused when the inductor current reaches zero during the dead-time.

The authors have been proposed a non-liner transmission power error compensation method using a three-level operation [9-10]. The voltage polarity reversal phenomenon is avoided by designing a zero current phase to be longer than the dead-time using three-level operation. However, the compensation method for the DC-bus voltage variation does not include the previous consideration. In actual energy storage systems for the DC micro-grid, the voltage fluctuation should be considered because the DC-bus voltage is varied according to the power generation of photovoltaic systems and load conditions.

This paper proposes the transmission power error compensation method corresponding to the voltage variation on each DC-bus. By applying the proposed method, the operation range of energy storage systems are expanded because the transmission power error is compensated. The new contribution of this paper is to overcome the problems of the conventional compensation method that is the transmission power error due to the variation of the inverter input voltage.

This paper is organized as follows; firstly, a dead-time effect for the transmission power is introduced. Secondly, the non-linear dead-time compensation method for the variable DC-bus voltage is explained. Finally, experiments are conducted in order to verify the compensation method of the non-linear transmission power error due to the dead-time when the DC-bus voltage is varied.

II. DEAD-TIME EFFECT FOR TRANSMISSION POWER

Figure 1 shows the circuit configuration of the DAB converter. The DAB converter is constructed from two full bridge inverters and a high frequency transformer. Each inverter outputs the square wave voltage with the duty of 0.5 and the transmission power is controlled by the phase-shift between the primary and secondary side of the inverter output voltage.

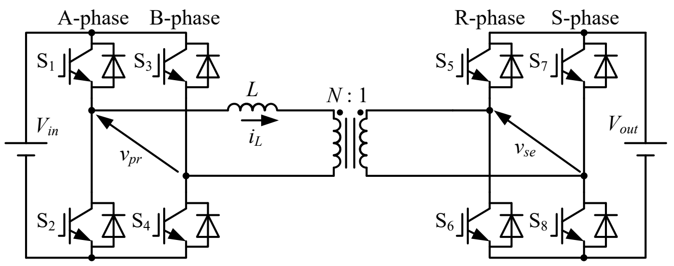

Fig. 1. Dual active bridge converter.

Figure 2 shows operation waveforms of two-level mode with and without the dead-time. Without considering the dead-time, the transmission power is controlled by the phase-shift without transmission power error. From Fig. 2 (a), the inductor current is expressed as (1) taking no account of the parasitic capacitance and the magnetizing current. Note that the turn ratio N is regarded as one for simplify considering in this paper.

$$i_L(\theta)=\begin{cases}\dfrac{V_{in}+V_{out}}{\omega L}\theta-\dfrac{1}{2\omega L}\{\pi V_{in}+(2\delta-\pi)V_{out}\} \\ \qquad for\ \ (0\le\theta\le\delta) \\ \dfrac{V_{in}-V_{out}}{\omega L}(\theta-\delta)+\dfrac{1}{2\omega L}\{(2\delta-\pi)V_{in}+\pi V_{out}\} \\ \qquad for\ \ (\delta\le\theta\le\pi)\end{cases} \qquad (1),$$

where V_{in} and V_{out} are an input voltage and an output voltage, ω is a switching angular frequency, L and δ are an additional inductor and δ phase-shift between the primary inverter output voltage v_{pr} and the inverter on the secondary side output voltage v_{se}. According to (1), the transmission power is given by (2),

$$P=\frac{V_{in}V_{out}}{\omega L}\delta\left(1-\frac{|\delta|}{\pi}\right) \qquad (2).$$

Meanwhile, the dead-time is necessary in order to prevent short circuit. The non-linear transmission error occurs when the inductor current becomes zero during the dead-time. The inductor current is clamped zero because the inductor current is not conducted during the dead-time. Consequently, the polarity of the inverter output voltage is reversed by the clamped inductor current. In addition, the transmission error is varied depends on the width of the voltage polarity reversal phenomenon. On the other hand, the linear dead-time error is caused by current direction during the dead-time. The polarity of the inductor current at the region A becomes negative at light load when the $V_{in} \neq V_{out}$. As the result, the diodes of the secondary side inverter does not conduct during the dead-time because the inductor current direction is different from the forward direction of the diodes. Thus, the transmission power has the error by the dead-time because the rise-timing of the secondary inverter output voltage is delay by the dead-time.

Figure 3 shows the relationship between the phase-shift and the transmission power when the output voltage is varied from 0% to -25%. The transmission power error is varied according to the fluctuation of the output voltage. In Fig. 3, the non-linear transmission error occurs when the output voltage is varied from 0% to -15%. In contrast, the linear error is caused when the output voltage is varied from -20% to -25%. Therefore, the dead-time compensation method corresponding fluctuation of the DC-bus voltage is required in order to compensate two types of dead-time effect.

Figure 4 shows the condition of occurrence of the transmission error due to the dead-time. The non-linear transmission power error occurs when the inductor current becomes zero during the dead-time. Therefore, the initial point of the voltage polarity reversal phenomenon is when the zero cross point of the inductor current equals the final point of the dead-time. This condition of the phase-shift is expressed by (3) using (1) of $0\le\theta\le\delta$,

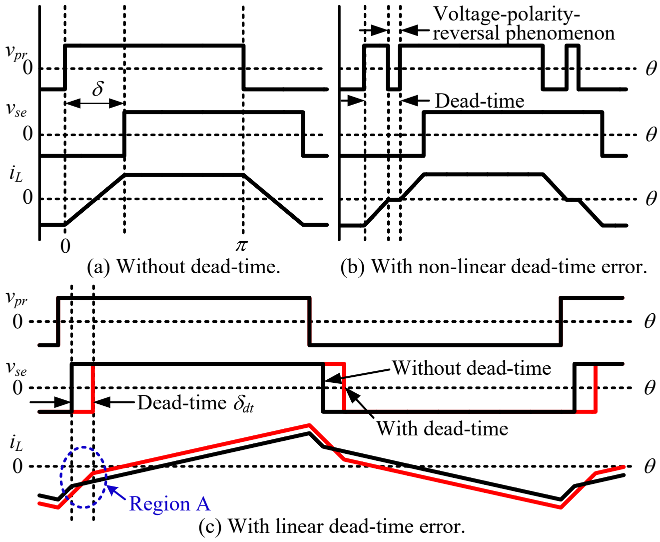

(a) Without dead-time. (b) With non-linear dead-time error.
(c) With linear dead-time error.
Fig. 2. Operation waveforms of two-level mode.

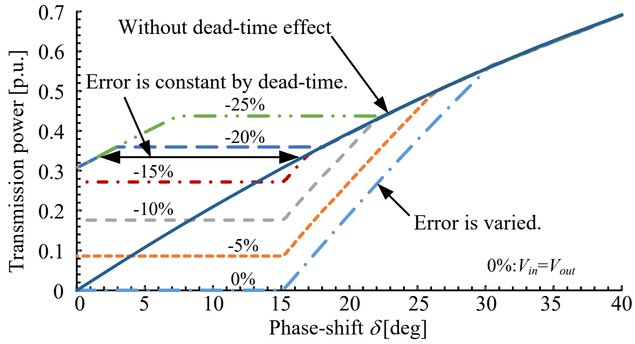

Fig. 3. Relationship between phase-shift and transmission power.

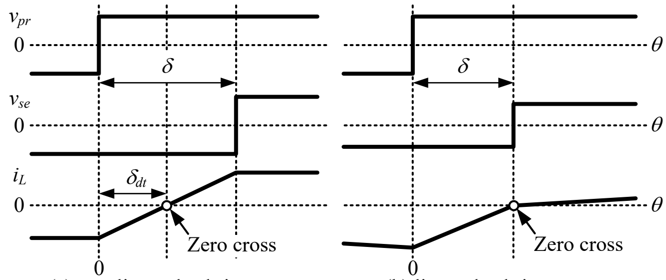

(a) non-linear dead-time error. (b) linear dead-time error.
Fig. 4. Condition of occurrence of transmission power.

$$\begin{gathered}\frac{V_{in}+V_{out}}{\omega L}\delta_{dt}-\frac{1}{2\omega L}\{\pi V_{in}+(2\delta-\pi)V_{out}\}\ge 0 \\ \delta\le(2\delta_{dt}-\pi)\frac{V_{in}}{2V_{out}}+\frac{1}{2}(2\delta_{dt}+\pi)\end{gathered} \qquad (3).$$

In addition, the condition of ratio between input and output voltage is expressed by (4) form (3),

$$\frac{V_{in}+V_{out}}{\omega L}\delta_{dt}-\frac{1}{2\omega L}\{\pi V_{in}+(2\delta_{dt}-\pi)V_{out}\}\ge 0$$
$$\frac{\pi-2\delta_{dt}}{\pi}\le\frac{V_{out}}{V_{in}}=\alpha \qquad (4),$$

where α is the rate of the fluctuation of the output voltage that is calculated as V_{out} / V_{in}. On the other hand, the linear transmission power error occurs when the polarity of the inductor current becomes negative as illustrated Fig. 2 (c). Therefore, the initial point of the linear transmission error is expressed by Fig. 4 (b). From Fig. 3 (b), the condition of the occurrence of the linear transmission error is given by (5) using (1) of $\delta\le\theta\le\pi$,

$$\frac{1}{2\omega L}\{(2\delta-\pi)V_{in}+\pi V_{out}\}\le 0$$
$$\delta\le\frac{V_{in}-V_{out}}{2V_{in}}\pi \qquad (5).$$

III. Non-Linear Transmission Power Error Compensation Method

Figure 5 shows the operation waveform of the three-level mode. From Fig. 5, the inductor current is given by (6) under the steady state condition,

$$i_L(\theta)=\begin{cases}-\frac{1}{2\omega L}\{V_{in}(\pi-2\varepsilon)-V_{out}(\pi-2\gamma)\} \\ \quad for\ (0\le\theta\le\varepsilon) \\ \frac{V_{in}}{\omega L}(\theta-\varepsilon)-\frac{1}{2\omega L}\{V_{in}(\pi-2\varepsilon)-V_{out}(\pi-2\gamma)\} \\ \quad for\ (\varepsilon\le\theta\le\delta+\gamma) \\ \frac{(V_{in}-V_{out})}{\omega L}(\theta-\delta-\gamma)-\frac{1}{2\omega L}\{V_{in}(2\delta+2\gamma-\pi)+V_{out}(\pi-2\gamma)\} \\ \quad for\ (\delta+\gamma\le\theta\le\pi-\varepsilon) \\ -\frac{V_{out}}{\omega L}(\theta-\pi+\varepsilon)+\frac{1}{2\omega L}\{V_{in}(\pi-2\varepsilon)+V_{out}(2\varepsilon+2\delta-\pi)\} \\ \quad for\ (\pi-\varepsilon\le\theta\le\delta+\pi-\gamma) \\ \frac{1}{2\omega L}\{V_{in}(\pi-2\varepsilon)+V_{out}(2\gamma-\pi)\} \\ \quad for\ (\delta+\pi-\gamma\le\theta\le\pi)\end{cases} \qquad (6).$$

From (6), the transmission power P is given by (7),

$$P=\frac{2}{2\pi}\int_0^{\pi}v_{pr}(\theta)i_L(\theta)d\theta$$
$$=\frac{V_{in}V_{out}}{2\pi\omega L}\{(\pi-2\gamma)(\delta-\varepsilon+\gamma)-(\delta+\varepsilon-\gamma)(\delta+\varepsilon+\gamma-\pi)\} \qquad (7),$$

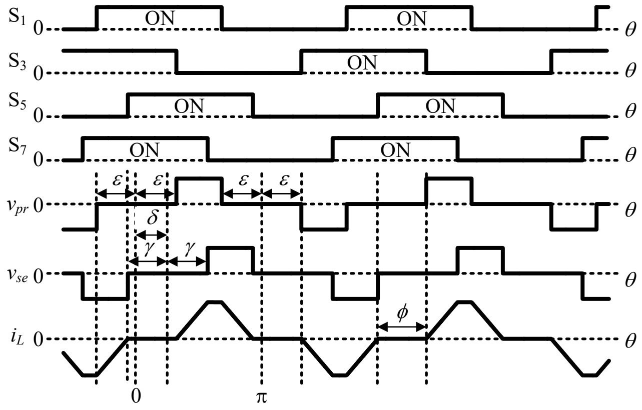

Fig. 5. Operation waveforms of three-level mode.

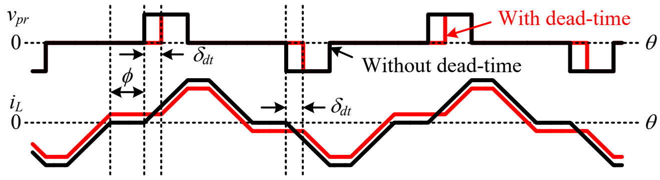

Fig. 6. Dead-time effect of three-level mode.

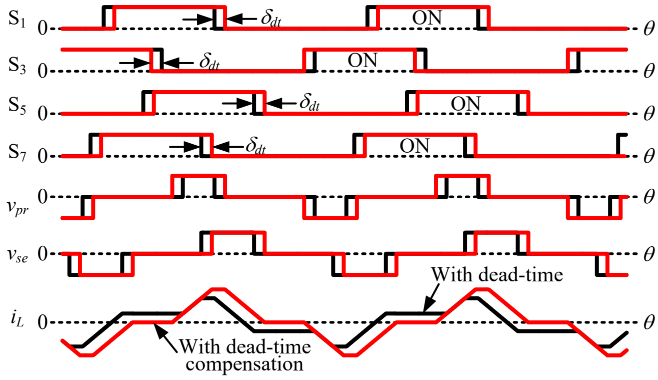

Fig. 7. Duty compensation for primary inverter output voltage.

where ε and γ are the zero voltage period of the primary and secondary side inverter output voltage. By applying this three-level operation, the voltage polarity reversal phenomenon is avoided by designing the zero current period ϕ to be longer than the dead-time because the voltage polarity reversal phenomenon is caused when the inductor current reaches zero during the dead-time. The condition of avoiding the voltage polarity reversal phenomenon is expressed by (8),

$$\varphi=\gamma+\varepsilon-\delta\ge\delta_{dt} \qquad (8).$$

Figure 6 shows the dead-time effect of three-level mode. The duty of the inverter output voltage of the primary side is decreased by the dead-time because diodes of the B-phase leg is not conducted during the dead-time instead of designing the zero-current period to be longer than the dead-time. Therefore, the duty of the primary inverter output voltage is needed to be compensated.

Figure 7 shows the duty compensation for the primary inverter output voltage. The duty error by the dead-time is compensated by (9) because the decrease of the duty affects the phase-shift δ and the zero voltage phase ε,

$$\begin{cases} \delta^* = \delta + \frac{1}{2}\delta_{dt} \\ \varepsilon^* = \varepsilon - \frac{1}{2}\delta_{dt} \\ \gamma^* = \gamma \end{cases} \quad (9),$$

where δ^*, ε^* and γ^* are the phase-shift commands, the zero voltage period command of the primary and secondary inverter.

IV. Transmission Power Error Compensation Method for Variable DC-bus Voltage

Figure 8 shows the operation waveforms of the three-level mode by applying the conventional method in [9-10] when the output voltage is varied. The voltage polarity reversal phenomenon occurs because the zero current period is not designed to be longer than dead-time due to the voltage fluctuation. In addition, the inductor current is increased by the circulating current. Therefore, the transmission power error compensation method for the variable voltage is required.

Figure 9 shows the operation waveforms of the proposed three-level modes. This compensation method is applied three-types of the three-level operation due to avoid the voltage polarity reversal phenomenon. In order to design the zero current period in the three-level operation, the initial value of (6) for $\varepsilon \leq \theta \leq \delta + \gamma$ need to be zero. This condition is expressed by (10) with $V_{out} = \alpha V_{in}$,

$$\begin{aligned} V_{in}(\pi - 2\varepsilon) - \alpha V_{in}(\pi - 2\gamma) = 0 \\ 2\varepsilon = 2\alpha\gamma + (1-\alpha)\pi \end{aligned} \quad (10).$$

A. Three-level mode I

In order to reduce the RMS value of the inductor current, the circulating current is need to be suppressed. The circulating current is reduced by suppressing the phase-shift angle and zero-voltage periods regarding the transmission power. The phase-shift and zero-voltage periods are minimized when the zero-current period ϕ is the same as the dead-time δ_{dt} [10]. The condition of $\phi = \delta_{dt}$ is given by (11), using (8) and (10),

$$2\gamma = \frac{2}{(\alpha+1)}\left\{\delta + \delta_{dt} - (1-\alpha)\frac{\pi}{2}\right\} \quad (11).$$

From (10) and (11), the transmission power is controlled by only the control variable of the phase-shift δ. In this mode, the voltage polarity reversal phenomenon occurs when the secondary zero voltage period γ becomes dead-time δ_{dt}. Therefore, the control limit of the three-level mode I is expressed by (12) from (11),

$$\delta \leq \frac{1}{2}(1-\alpha)(\pi - \delta_{dt}) \quad (12).$$

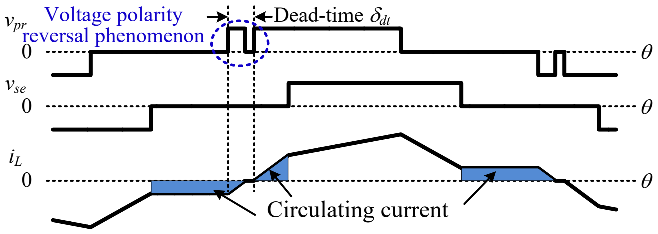

Fig. 8. Operation waveforms of three-level mode by applying conventional method.

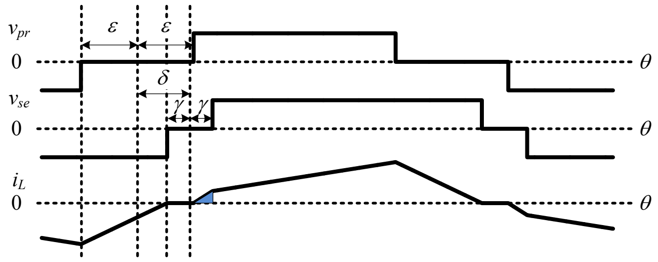

(a) Mode I.

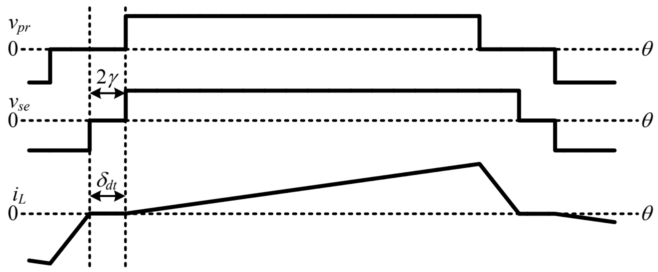

(b) Mode II.

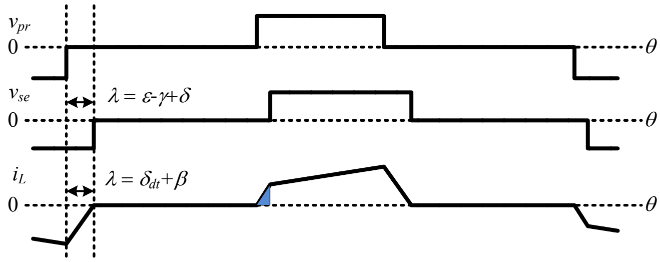

(c) Mode III.

Fig. 9. Operation waveforms of the proposed three-level modes.

B. Three-level mode II

In the three-level mode II, the transmission power is controlled by the secondary zero voltage period γ. In order to control one control variable of the secondary zero voltage period γ with suppressing the circulating current, the phase-shift δ is designed as fixed value of (12) in the equality condition. In the case of controlling the zero-voltage period γ with the fixed phase-shift δ, the phase-difference λ in Fig. 6 (b) needs to satisfy (13) in order to avoid the voltage-polarity-reversal phenomenon,

$$\lambda = \varepsilon - \gamma + \delta > \delta_{dt} \quad (13).$$

According to (10), (12), and (13), the secondary zero-voltage-period γ is limited by (14),

$$\gamma \le \frac{3-\alpha}{2(\alpha-1)}\delta_{dt} + \pi \tag{14}$$

C. Three-level mode III

After the operating region of the three-level mode II, the three-level mode III is applied. In order to avoid the voltage polarity reversal phenomenon, the phase-difference λ is designed to $\lambda=\delta_{dt}+\beta$ where β is a few margin to avoid the voltage-polarity-reversal phenomenon. The margin β is needed to be design as small as possible because the circulating current increases as the margin β is larger. When an FPGA is used for an experiment, the margin β is determined as one clock of the FPGA because the phase-shift is controlled by the clock period of the FPGA. The condition of achieving $\lambda=\delta_{dt}+\beta$ is obtained by (15) using (10) and (13),

$$\delta = \delta_{dt} + \beta + (1-\alpha)\left(\gamma - \frac{\pi}{2}\right) \tag{15}$$

Figure 10 shows the flowchart of the determination of operation modes. The operation mode is determined as follows; in order to decide whether the operating point is in the dead-time effect area or not, the phase-shift angle δ is calculated with the transmission power command P^* by solving (2) for the phase-shift δ,

$$\delta = \frac{\pi - \sqrt{\pi^2 - \dfrac{4\pi\omega L P^*}{V_{in}V_{out}}}}{2} \tag{16}$$

Next, the kind of the dead-time effect is decided from the voltage ratio α using (4). The non-linear transmission error is compensated when the voltage ratio satisfies (4). On the other hand, the linear transmission error is compensated when the voltage ratio does not satisfy (4). After the decision of the kind of the dead-time effect, the operation mode is selected from the two-level mode or three-level modes using (3) in the non-linear dead-time effect flow. In contrast, in the linear dead-time effect flow, the operation mode is determined by (5). The three-level operation is applied if the phase-shift δ satisfies the (3) or (5). The three-level modes is decided by (12) and (14). The three-level mode II is applied when the phase-shift δ is not satisfy (12). In addition, the three-level mode III is used when the secondary zero voltage period γ is not satisfy (14). In the linear dead-time effect flow, the three-level mode III is not necessary because the secondary zero voltage period γ satisfies (14) until -25% of the voltage fluctuation. Finally, the duty of the inverter output voltage is compensated by (9) when the three-level operation is applied.

Table I. Experimental specifications.

Quantity	Symbol	Value
Input voltage	V_{in}	240 V
Output voltage	V_{out}	240-180 V
Rated power	P	1.9 kW(45 deg)
Dead time	T_{dt}	2.1 μs (15 deg)
Additional inductance	L	128 μH
Turn ratio of transformer	N	1
Switching frequency	f_{sw}	20 kHz
Margin of dead time	β	0.36 deg

V. Experimental Results

Table I shows the experimental specifications. A 1.9-kW prototype of the DAB converter was tested in order to confirm the validity of the proposed method. In this experiment, the output voltage is regarded as the high voltage DC-bus. Therefore, the proposed transmission power compensation method for the voltage fluctuation was confirmed by varying the output voltage.

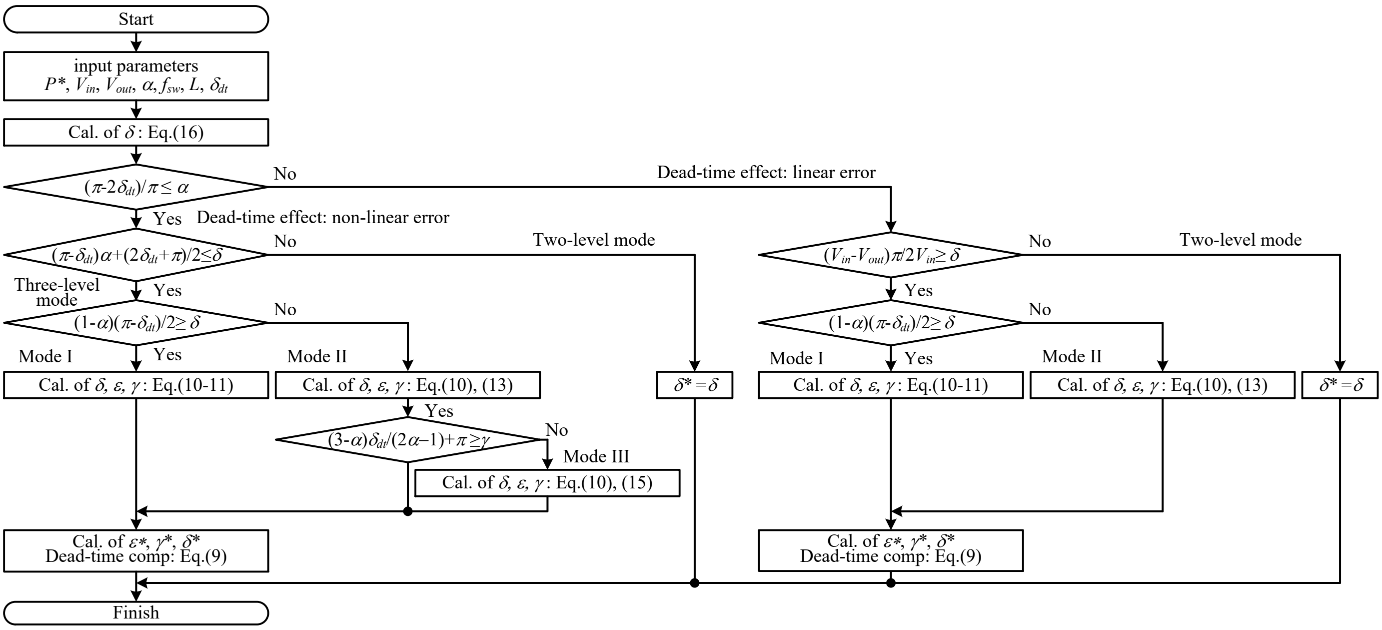

Fig. 10. Flowchart of determination of operation modes.

Figure 11 shows the operation waveforms of the two-level mode and three-level mode when the output voltage fluctuation is -10%. The voltage-polarity-reversal phenomenon occurs when the conventional two-level mode is applied. In contrast, by applying the proposed method, the voltage-polarity-reversal phenomenon is avoided by controlling the zero voltage period individually.

Figure 12 shows the characteristics of the transmission power regarding the transmission power command when the output voltage is varied to -10% and -15%. According to Fig. 12 (a), by applying the proposed method, the transmission-power error is reduced from 49% to 3.5% by avoiding the voltage-polarity-reversal phenomenon. The transmission power error of the proposed method at 0.2p.u. is caused by the error of the zero-voltage phase due to a parasitic capacitor. In the proposed method, switches S3 and S4 do not achieve zero voltage switching (ZVS), whereas zero current switching (ZCS) is achieved at 0.2p.u. because a turn-on timing of primary and secondary inverter output voltages is same. Hence, the rise time of the inverter output voltage is delay by the time constant of the parasitic capacitor because the parasitic capacitance is not discharged. Fig. 12 (b) shows the transmission power characteristic when the output voltage is varied to -15%. In the two-level mode, the dead-band occurs due to the dead-time. In contrast, the dead-band is suppressed by proposed the transmission power compensation method.

VI. Conclusion

This paper proposed the compensation method of transferred power error due to the dead-time when the for variable DC-bus voltage. The voltage polarity reversal phenomenon was avoided by designing the zero current period to be longer than the dead-time. In order to avoid the voltage polarity reversal phenomenon under the voltage fluctuation, three-types of three-level modes were proposed. From the experimental results, the error of the transmission power was reduced from 49% to 3.5% because the voltage-polarity-reversal phenomenon was avoided.

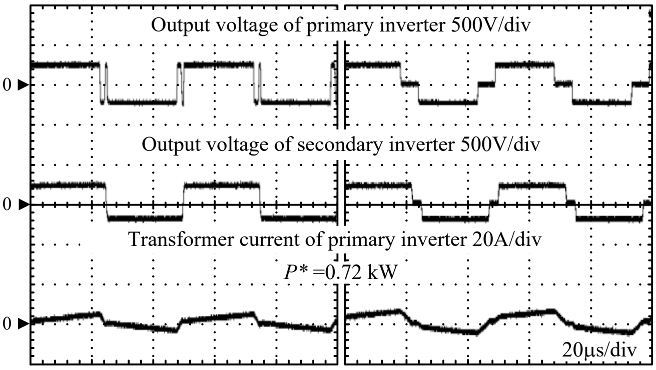

Fig. 11. Operation waveforms of three-level mode by applying conventional method.

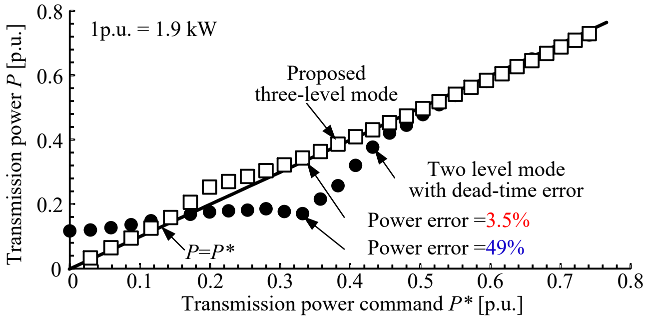

(a) Outout voltage condition is reduced by -10% from nominal value.

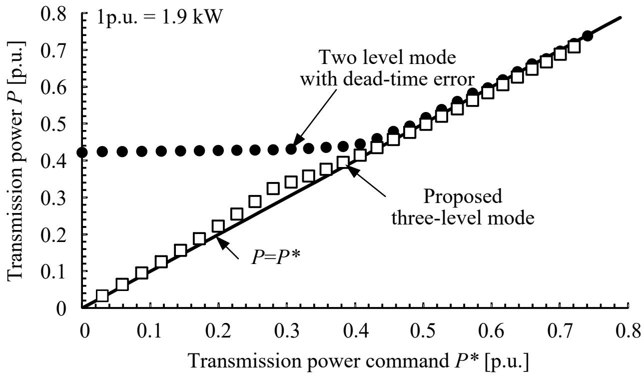

(b) Outout voltage condition is reduced by -15% from nominal value.

Fig. 12. Characteristics of transmission power regarding transmission power command

References

[1] M. Mao, Z. Dong, L. Chang: "Accurate Output Power Control of Converters for Microgrids Based on Local Measurement and Unified Control", IEEJ Journal of Industry Applications, Vol. 4, No. 4, pp.331-338, 2015.

[2] H. Kakigano, Y. Toshifumi: "Low-Voltage Bipolar-Type DC Microgrid for Super High Quality Distribution", IEEE Trans. on Power Electronics, Vol. 25, No. 12, pp.3066-3075, 2010.

[3] J. M. Guerrero, J. C. Vasquex, J. Matas, L. G. Vicuna, M. Castilla: "Hierarchical Control of Droop-Controlled AC and DC Microgrids—A General Approach Toward Standardization", IEEE Trans. on Industry Applications, Vol. 58, No. 1, pp.158-172, 2011.

[4] G. Guidi, A. Kawamura, Y. Sasaki and T. Imakubo, "Dual active bridge modulation with complete zero voltage switching taking resonant transitions into account," Proceedings of the 2011 14th European Conference on Power Electronics and Applications, Birmingham, 2011, pp. 1-10.

[5] Felix J. and Jurgen B., "Generalized Modeling and Optimization of a Bidirectional Dual Active Bridge DC-DC Converter Including Frequency Variation", IEEJ Journal of Industry Applications, Vol.4, No.5, pp.593-601, 2015.

[6] M. Nakahara, K. Wada: "Loss Analysis of Magnetic Components for a Solid-State-Transformer", IEEJ Journal of Industry Applications, Vol. 4, No. 4, pp.387-394, 2015.

[7] H. Higa and J. Itoh, "Extension of zero-voltage-switching range in dual active bridge converter by switched auxiliary inductance," 2017 IEEE Energy Conversion Congress and Exposition (ECCE), Cincinnati, OH, 2017, pp. 5324-5331.

[8] B. Zhao, Q. Song, W. Liu, Y. Sun: "Dead time Influence of the High-Frequency Isolated Bidirectional Full-Bridge DC-DC Converter: Comprehensive Theoretical Analysis and Experimental Verification", IEEE Trans. on Power Electronics, Vol. 29, No. 4, pp.1667-1680, 2014.

[9] J. Itoh, K. Kawauchi, H. Higa " Dead-time Compensation with DC Offset Current Elimination Method using Three-level Operation for Dual Active Bridge DC-DC Converter," 2018 IEEE Energy Conversion Congress and Exposition (ECCE), Portland, OR, pp. 6299-6306, 2018.

[10] J. Itoh, K. Kawauchi, H. Watanabe, K. Kusaka " Reduction of Transmission Power Error and Current for Dual Active Bridge DC-DC Converter in Energy Storage Systems," 7th International Conference on Renewable Energy Research and Applications (ICRERA 2018), 2018.